environments

MDPI

Article

An Open Source GIS-Based Application for the Assessment of Groundwater Vulnerability to Pollution

Lia Duarte [1,2,*], Jorge Espinha Marques [1,2] and Ana Cláudia Teodoro [1,2]

1 Department of Geosciences, Environment and Land Planning, Faculty of Sciences, University of Porto, 4169-007 Porto, Portugal
2 Earth Sciences Institute (ICT), Faculty of Sciences, University of Porto, 4169-007 Porto, Portugal
* Correspondence: liaduarte@fc.up.pt; Tel.: +351-220402477

Received: 27 June 2019; Accepted: 19 July 2019; Published: 21 July 2019

check for updates

Abstract: Groundwater is a crucial natural resource for regular socio-economic function. Groundwater vulnerability to pollution can be assessed through Geographical Information System (GIS)-based qualitative methods. GIS-based tools, dedicated to the assessment of groundwater vulnerability, usually present several limitations, such as high cost, unavailable code, and a lack of functionality concerning the flexible application of vulnerability indices and vulnerability map comparison. The objective of this work was to create a new GIS-based open source application for groundwater vulnerability assessment, *GVTool*, developed using QGIS software, with the capability of creating and comparing groundwater vulnerability maps considering four different methods: DRASTIC, GOD, SINTACS, and Susceptibility Index (SI). This application incorporates features from a previous tool, *DRASTIC Model*, and new functionalities were included, namely three additional vulnerability assessment methods, map comparative analysis, map statistics, and index interval reclassification and symbology definition. The *GVTool* functionalities and capabilities are illustrated through a groundwater vulnerability assessment in Serra da Estrela mountain (Central Portugal). *GVTool* is mostly useful in integrated assessments, helping to verify if the groundwater vulnerability maps are accurate and to decide which is the most suitable method or the combination of methods to express groundwater vulnerability to pollution in a specific area.

Keywords: QGIS; water resources; vulnerability index

1. Introduction

Groundwater is a crucial natural resource for regular socio-economic function. The occurrence of potable groundwater is widespread, and, for that reason, it is an essential source of water supply worldwide. Groundwater provides more than 40% of the world's irrigation water and around 50% of municipal water extractions [1].

The estimated worldwide groundwater abstraction is around 982 km^3/year, corresponding to around a quarter of the total water abstraction. Of this groundwater volume, 70% is for irrigation, 21% is for domestic use, and the remainder is mostly for industrial use [2].

In several countries, the deficient access of populations to appropriate water supplies causes severe socio-economic vulnerability, and consequently, poverty. However, it is possible to promote water poverty to water prosperity through the sustainable exploitation of groundwater from high-quality, relatively low-cost, drought-resilient aquifers [3].

During the last decades, an increasing global awareness regarding the key ecological, hydrological, and economic roles of groundwater bodies has driven both national and international authorities to create instruments intended to protect aquifer systems from pollution and assure the normal provision of ecosystem services. A good example of such practices are fundamental norms included in European river basin management plans, as required by the Water Framework Directive and by the Groundwater Directive of the European Union [4–7].

The assessment of groundwater vulnerability to pollution is a major hydrogeological topic that faces a number of constraints, namely, the great complexity of groundwater systems resulting from the occurrence of three-dimensional groundwater flow and pollutant transport through heterogeneous and anisotropic geologic materials, often coupled with the poorly known nature and spatial distribution of pollution sources [8,9].

Van Duijvenbooden and Waegeningh [10] define groundwater vulnerability to pollution as the sensitivity of groundwater quality to an imposed pollutant load, which is determined by the intrinsic characteristics of the aquifer. The intrinsic groundwater vulnerability, which cannot be clearly quantified by means of a standardized method, encompasses the properties of hydrogeological systems that control the subsurface water circulation through the unsaturated zone and the aquifer, and therefore, also determine the risk of a pollutant to reaching groundwater [8,11].

On the other hand, specific vulnerability also considers the properties of a contaminant, namely, its load, time of impact, as well as the spatial features of the pollution source [11–13].

In general terms, groundwater vulnerability to pollution can be assessed considering three types of methods [14]: (i) Geographical Information System (GIS)-based qualitative methods; (ii) process-based methods; and (iii) statistical methods (which encompass artificial intelligence methods). Intrinsic vulnerability can be assessed by using GIS-based qualitative methods and statistical methods.

GIS-based qualitative methods based on the subjective rating of hydrogeological factors are commonly used to evaluate groundwater vulnerability, because these methods are relatively simple to employ, inexpensive, less time-demanding, and are often suitable for application in situations of data scarcity [14,15]. Furthermore, the application of such methods is useful as a decision-making instrument for sustainable management of water resources, as well as for land-use planning. However, a number of downsides are pointed out for GIS-based qualitative methods, such as the subjective nature of vulnerability evaluation, the possibility of relying on simplistic hydrogeological characterizations, the lack of a physical basis, and the difficulty of evaluating the accuracy of results, and in many cases, of delimiting areas with different levels of vulnerability to pollution [8,14]. Some of the most common methods are: DRASTIC [16], GOD [17], System for Early Evaluation of Pollution potential from Agricultural Groundwater Environments (SEEPAGE) [18], Aquifer Vulnerability Index (AVI) [19], SINTACS [20,21], EPIK [22], ISIS [23], KARSTIC [24], and Susceptibility Index (SI) [25].

Given the fundamental role of safe water supply and the technical difficulties and high costs of aquifer remediation operations, pollution prevention is the most adequate strategy in sustainable management of groundwater resources [26]. For that purpose, the application of groundwater vulnerability indices coupled with GIS analysis is a valuable and cost-efficient approach to identify and help protect the most vulnerable areas at various scales [27,28].

In fact, GIS allows one to generate, manipulate, analyze, and visualize geographic information in a flexible and integrated manner. This is achieved by using several layers of information and large data sets, thus meeting the requirements of complex hydrogeological conceptual models, which often require a holistic and transdisciplinary perspective in order to obtain an accurate representation of the spatial variability of groundwater vulnerability. GIS is also useful in overcoming other issues in the assessment of groundwater vulnerability, including: (i) the need to compare the results obtained by applying different indices, highlighting the advantages and disadvantages of each method [29,30]; (ii) the combination of different indices in order to obtain more realistic results representing separately, for instance, the vulnerability conditions in the topsoil, the unsaturated zone, and the aquifer [31].

GIS-based tools for the assessment of groundwater vulnerability are scarce and usually do not address fundamental issues, specifically: (i) to provide a user-friendly software that overcomes the high-cost and low flexibility of proprietary software, without compromising the code's reliability; (ii) to allow adaptations to groundwater vulnerability indices, namely, by changing the factor's weights and ratings; and (iii) to allow detailed vulnerability map comparisons. In most of the cases described in the literature, the assessment of intrinsic groundwater vulnerability is carried out using GIS proprietary software to produce vulnerability index maps [32–36]. For instance, Oroji [30] used proprietary software to assess groundwater vulnerability through DRASTIC and GOD indices in the Asadabad plain. Yousefi et al. [33] also used proprietary software to estimate DRASTIC and SINTACS methods in the Khorramabad-Lorestan Plain, western Iran.

However, open source and free applications have significant benefits, namely, the free distribution and the public availability of the code, which can be modified by any user [37]. QGIS is one of the most popular GIS open source software programs, with the important advantage of making the development of plugins using Python language easy and quick [38]. QGIS integrates external algorithms from other software, which complements itself.

Some GIS open source applications for QGIS involving groundwater vulnerability methods have been developed so far; for instance, the *Groundwater Vulnerability Mapping* plugin, hosted in the QGIS official repository [39], and the *PaPRIKa* QGIS plugin [40]. Rossetto et al. [41] also developed the FREE and open source software tools for WATer resource management (FREEWAT) platform, a free and open source software integrated in QGIS for planning and management of water resources, with specific attention to groundwater. Duarte et al. [42] developed a GIS open source application under QGIS open source software, named *DRASTIC Model*, which allows automatic creation of groundwater vulnerability maps within a friendly graphic interface.

The objective of this work was to present a new GIS open source application for the assessment of groundwater vulnerability to pollution—the Groundwater Vulnerability Tool (*GVTool*). This application incorporates features from *DRASTIC Model* and adds three more GIS-based qualitative methods: GOD, SINTACS, and SI. Also, new functionalities were included: (i) *Comparative Analysis,* allowing one to perform more detailed comparisons between different groundwater vulnerability maps; (ii) *Symbology* to reclassify the symbology of the maps; and (iii) *Map Statistics* to estimate the statistics of the resulting maps. Therefore, the user can evaluate the weaknesses and strengths of each method and decide which is the most suitable method to represent groundwater vulnerability in a specific study area.

2. Materials and Methods

2.1. QGIS Open Source Software

GVTool open source application was developed using a previous version as the base, also created under QGIS open source software—the *DRASTIC Model* [42]. In *DRASTIC Model*, several open source libraries were used in the application development, such as QGIS Application Programming Interface (API), Gdal/OGR API, and PyQt API. In *GVTool*, the libraries were updated to Python 3. In *GVTool*, QGIS version 3.4 was used and Python 2 was replaced by Python 3. In QGIS 3.0, *Processing Toolbox* has been refactored and it is much more powerful than in QGIS 2.0 [43]. QGIS 2.0 was released in 2013, and since then updated versions were also released up until 2.18. QGIS 3.0 was introduced with new API libraries, such as Qt 5 and Python 3. This improvement was mandatory to overcome limitations and issues not fixed in version 2.0. The disadvantage of this update was the fact that all the plugins developed in QGIS version 2 no longer function in QGIS 3.0. The *DRASTIC Model* application, which was developed in QGIS 2.0, was updated to QGIS 3.0 (in this case, QGIS 3.4), so all the code was rewritten.

GVTool is a new application, with substantially improved capabilities, incorporating additional functionalities (Figure 1):

1. besides the DRASTIC vulnerability index, the application includes GOD, SINTACS, and SI methods;
2. a *Comparative Analysis* menu, which provides the users several alternatives to compare groundwater vulnerability maps obtained by applying different methods to the same area;

3. a *Map Statistics* menu capable of performing statistical analysis of a raster;
4. a *Symbology* menu was created to provide the user the capability of redefining vulnerability classes and to apply the respective symbology to a map or a set of maps.

The main purpose of applying *GVTool* is to calculate the groundwater vulnerability value for each grid cell defined in the study area map, according to one of the implemented methods (DRASTIC, GOD, SI, or SINTACS). The *Help* menu was updated with information regarding all of the implemented indices.

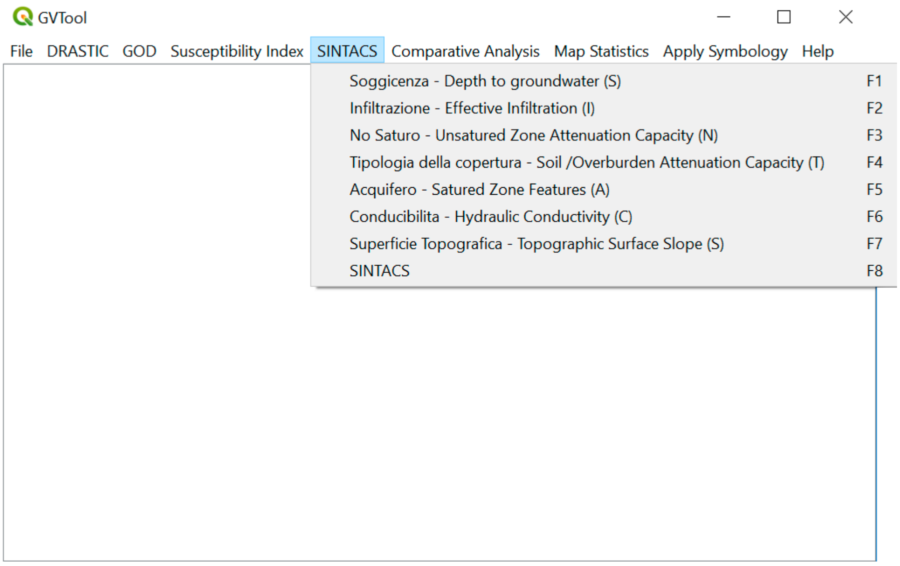

Figure 1. *GVTool* main window.

2.2. Implemented Groundwater Vulnerability Assessment Methods

Three of the implemented methods (DRASTIC, GOD, and SINTACS) are well established, and could be applied in most hydrogeological backgrounds. A fourth method, SI, was added because the resulting vulnerability maps express the effect of different land use classes, which could be a valuable feature in several situations.

2.2.1. DRASTIC

DRASTIC index [16] is the most well-known method for assessing groundwater vulnerability to pollution at municipal, national, and even continental scales [44,45]. The acronym DRASTIC stands for seven factors that control groundwater vulnerability according to Aller et al. [16]: Depth to Groundwater (D), Net Recharge (R), Aquifer Media (A), Soil Media (S), Topography (T), Impact of the vadose zone (I), and Hydraulic Conductivity (C). The DRASTIC index values are calculated from the sum of seven products according to the following expression (Equation (1)):

$$\mathrm{DRASTIC} = \mathrm{D}_w\mathrm{D}_r + \mathrm{R}_w\mathrm{R}_r + \mathrm{A}_w\mathrm{A}_r + \mathrm{S}_w\mathrm{S}_r + \mathrm{T}_w\mathrm{T}_r + \mathrm{I}_w\mathrm{I}_r + \mathrm{C}_w\mathrm{C}_r \quad (1)$$

where D, R, A, S, T, I, and C are the seven groundwater vulnerability factors; w and r are the weight and rating for each factor, respectively. Aller et al. [16] adopted a set of index intervals ranging from extremely low groundwater vulnerability (index value under 79) to extremely high groundwater vulnerability (index value higher than 200).

2.2.2. GOD

GOD index considers three groundwater vulnerability factors [17,46]:

1. the type of groundwater confinement (G factor), varying from 0 (corresponding to none or overflowing) to 1.0 (corresponding to unconfined);

2. the characteristics of the overlying strata (O factor), namely, the lithological character and degree of consolidation of the vadose zone or the confining beds (ranging from 0.4 in the case of lacustrine/estuarine clays to 1.0 in the case of karst limestones);
3. the D factor encompasses depth to groundwater table (for unconfined aquifers) or to groundwater strike (for confined aquifers), ranging from 0.6 (depth greater than 50 m) to 1.0 (for all depths in the case of karstic aquifers). The GOD index is calculated through the multiplication of these three factors (Equation (2)):

$$\mathrm{GOD} = \mathrm{G} \times \mathrm{O} \times \mathrm{D} \tag{2}$$

The results range from 0 (negligible vulnerability) to a maximum of 1.0 (extreme vulnerability).

2.2.3. SINTACS

The SINTACS method [20,21], was also derived from DRASTIC, but considers a more flexible way of selecting ratings and weights, through intervals or graphical representation of curves. This method evaluates groundwater vulnerability by means of seven factors identified in Italian: *Soggienza*—depth to groundwater (S); *Infiltrazione*—effective infiltration (I); *Non saturo*—unsaturated zone attenuation capacity (N), *Tipologia della copertura*—soil overburden attenuation capacity (T); *Acquifero*—saturated zone features (A), *Conducibilità*—hydraulic conductivity (C), and *Superficie topografica*—topographic surface slope (S).

The SINTACS index values are calculated in the same manner as DRASTIC, that is, as weighted sums of individual factors (Equation (3)):

$$\mathrm{SINTACS} = \mathrm{S}_r\mathrm{S}_w + \mathrm{I}_r\mathrm{I}_w + \mathrm{N}_r\mathrm{N}_w + \mathrm{T}_r\mathrm{T}_w + \mathrm{A}_r\mathrm{A}_w + \mathrm{C}_r\mathrm{C}_w + \mathrm{S}_r\mathrm{S}_w \tag{3}$$

where S, I, N, T, A, C, and S, are the groundwater vulnerability factors described previously, and w and r are the weight and rating for each factor, correspondingly.

Several SINTACS index intervals and the corresponding vulnerability classes have been defined. For example, Al Kuisi et al. [47] consider six intervals ranging from very low vulnerability (index value under 80) to very high vulnerability (index value higher than 210).

2.2.4. Susceptibility Index (SI)

The SI method is adapted from the DRASTIC method with the purpose of assessing groundwater vulnerability, at several scales, to diffuse agricultural pollution [25,48]. Besides using several vulnerability factors from the DRASTIC method, SI method adds a Land Use factor (LU). In this method, the factors I, S, and C from DRASTIC are absent and were replaced by the LU factor. Also, the weights in the parameters shared with DRASTIC are different. The SI index values are calculated from the sum of five products through the following expression (Equation (4)):

$$\mathrm{SI} = \mathrm{D}_w\mathrm{D}_r + \mathrm{R}_w\mathrm{R}_r + \mathrm{A}_w\mathrm{A}_r + \mathrm{T}_w\mathrm{T}_r + \mathrm{LU}_w\mathrm{LU}_r \tag{4}$$

where D, R, A, and T, are the same groundwater vulnerability factors used in DRASTIC, and LU is the land use factor; w and r are the weight and rating for each factor, respectively. According to Stigter et al. [25], the addition of the LU factor with the intention of considering agricultural pollution (namely, from fertilizers and pesticides) means that the SI is not a purely intrinsic vulnerability assessment method. Francés et al. [48] present the land use classes (defined in accordance with the Corine Land Cover map [49]) and the respective weights.

Stigter et al. [25] defined intervals ranging from extremely low groundwater vulnerability (index value under 30) to very high groundwater vulnerability (index value between 80 and 90).

Table 1 presents a summary of the no and low vulnerability values to high vulnerability values in the four presented indices (DRASTIC, GOD, SI, and SINTACS). As observed in # Table 1, the range of values are different regarding each method, so a normalization procedure is required in order to compare the methods.

Table 1. Summary of low to high vulnerability values in the indices.

Method	No-Vulnerability	High-Vulnerability
DRASTIC	<79	>200
GOD	0.0	1.0
SINTACS	<30	80–90
Susceptibility Index (SI)	<80	>210

3. Implementation of *GVTool*

GVTool is accessed through a button that opens a window comprising nine menus (Figure 1). The first menu allows one to open vector or raster files to the canvas. The next four menus correspond to the vulnerability index menus. The fifth menu (*Comparative Analysis*) allows one to perform detailed comparisons between the vulnerability maps generated in previous menus. The *Map Statistics* menu allows one to compute the statistics of a vulnerability map. The *Symbology* menu allows one to reclassify index values and to apply a specific symbology, defined by the user, to a specific map or sets of maps. The last menu includes the *help* related to the application.

In each vulnerability index menu, there are a certain number of buttons according to the methodology (Figure 1). Each button opens a window composed of a set of parameters to be defined. Some of the parameters are similar in all windows, such as inputs, cell size, extent, attributes, and outputs. The ratings can be defined in a table with the default descriptions of the method. However, the user can import the existing characteristics in the attribute table (always according to the attribute chosen) and then manually assign the ratings. In this respect, since *GVTool* shares some implementation features with *DRASTIC Model*, a more detailed explanation may be found in Duarte et al. [42]. The *GVTool* structure diagram is presented in Figure 2.

Some vulnerability factors, namely, depth to groundwater, net recharge, and topography rely on the creation of raster files. For this purpose, *GVTool*, similar to *DRASTIC Model*, computes pixel values through one of the following spatial interpolation methods: (i) inverse distance weighting [50]; (ii) Kriging [51]; (iii) cubic spline approximation [52]; or (iv) spatial approximation using spline with tension [53,54].

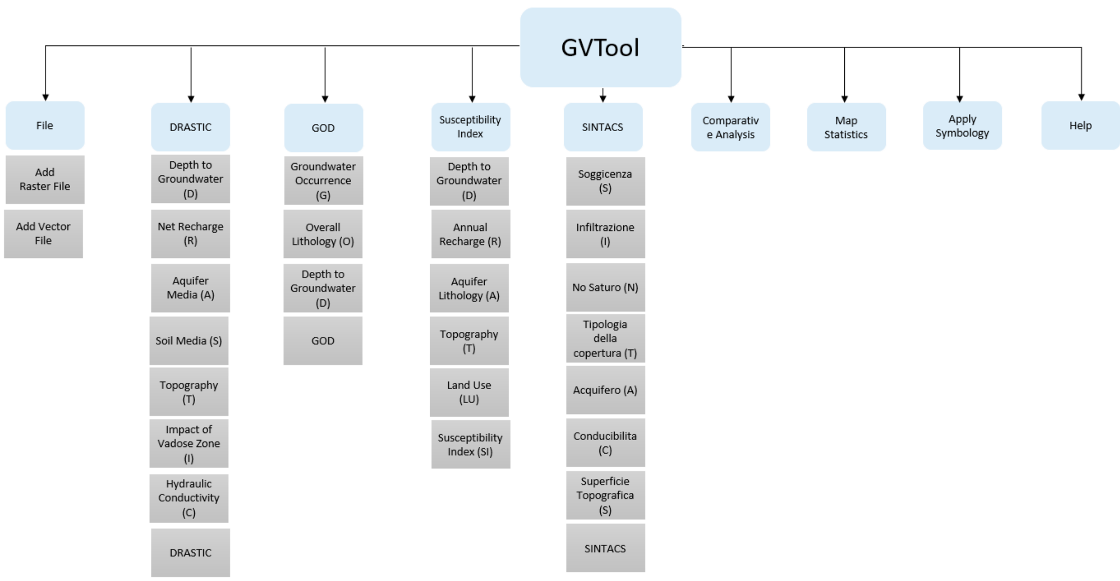

Figure 2. *GVTool* structure diagram.

3.1. Depth to Groundwater

The Depth to Groundwater factor is used in all four methods. It is defined as D in DRASTIC and GOD indices, G in SI, and S in SINTACS method. The code developed to implement the four indices was similar. However, in SINTACS there are not classes to modify (see Section 3.7). This factor represents the depth to the water table. The interface includes two methods: base and improvement. The base method is used when enough information regarding the depth to groundwater is available (usually water table depth values measured in wells). In this case, depth values are interpolated to create the corresponding raster. If this information is unavailable, the improvement method is applied, considering a Digital Elevation Model (DEM) and a simple hydrogeological conceptual model, which relies on the user knowledge on the local relation between depth to groundwater and landforms (as described in Duarte et al. [42]). The alternative method generates a surface through drainage network segments (rivers or streams) with values ranging from 0 m to a maximum depth value, which can be modified by the user. A distance raster is created from drainage network segment data. More information is available in Duarte et al. [42]. The depth to groundwater surface is created from drainage network segments, which are generated from DEM. In the D and G parameters, from DRASTIC and GOD, respectively, the same ratings are assigned. In the remaining parameters from GOD and SINTACS, the ratings are different.

3.2. Net Recharge

The Net Recharge factor is used in DRASTIC and SI as R, and in SINTACS as I. The implementation of this method was also similar in the first three cases, differing in SINTACS in the ratings and the implementation (see Section 3.7). The implemented methodology includes three methods, as described by Duarte et al. [42]: (i) in the base method the Net Recharge raster is obtained from a simplified water budget. which estimates recharge from precipitation, overland flow, and evapotranspiration; (ii) the second method relies on recharge rates available in regional hydrogeological studies and assumes that the spatial variability of this process is minor; and (iii) the third method may be applied in areas where the spatial variability of precipitation is mainly controlled by altitude and requires a regional recharge rate, a DEM, and a regression model expressing precipitation as a function of altitude.

3.3. Factors Related to Soil, to The Unsaturated Zone, and to Aquifer Features

The Aquifer factor is defined as Aquifer Media (A) in DRASTIC, Aquifer Lithology (A) in SI, and *Acquifero* (A) in SINTACS. The implemented methodology is similar in all cases. The user defines the ratings to each geological unit represented in the input shapefile, according to the geological map, in order to create a raster file. Each vulnerability index assigns its own ratings.

The Soil factor is defined as Soil Media (S) in DRASTIC and *Tipologia della copertura* (T) in SINTACS. The implementation is also similar in both methods, only differing in the ratings assigned. The functionality assigns the ratings to the input shapefile, according to the soil map, and a raster is created based on that information.

The LU graphic interface from SI method allows the possibility of importing the attribute table and to assign ratings according to the land cover classes represented in the input shapefile.

3.4. Topography

The Topography factor is used in DRASTIC and SI as Topography (T) and as *Superficie Topografica* (S) in SINTACS. The implemented methodology was similar in all methods, except in the ratings attribution in SINTACS, as explained in Section 3.7. The methodology implemented allows one to create a DEM from quoted points or to insert the DEM as an input. The Geographic Resources Analysis Support System (GRASS) algorithm *r.slope.aspect* was used to compute the slope map and the reclassification of the values was implemented through *reclassifyvalues* from System for Automated Geoscientific Analyses (SAGA). The assigned ratings are defined according to the method.

3.5. *Hydraulic Conductivity*

The Hydraulic Conductivity factor is used in DRASTIC as C and SINTACS as *Conducibilita* (C). The Hydraulic conductivity values may be available from previous regional studies and are inserted by the user in the respective attribute table for each geological unit. Alternatively, the user may apply typical values according to the geological materials occurring in the aquifers. Section 3.7 explains the implementation of C ratings in SINTACS.

3.6. *SINTACS Soggicenza, Infiltrazione, Conducibilita, and Superficie Topografica Factors*

The assignment of ratings in S, I, C, and S factors is different from the corresponding procedures adopted in the remaining vulnerability indices. The ratings are assigned based on curves defined for SINTACS [20,21]. The automatic assignment of ratings was carried out in several steps. First, the (x,y) coordinates of the points that compose the curve were obtained using the *Engauge Digitizer* open source software (http://markummitchell.github.io/engauge-digitizer/). Subsequently, a text file of the curve (x,y) coordinates was created and added to the application folder. The application can automatically read the input values and reclassifies the raster accordingly. The raster of each factor is then created with the assigned ratings. This process is the same for each factor, where the ratings are defined by a curve [20,21].

3.7. *Final Maps*

The final maps resulting from the application of groundwater vulnerability assessment methods are obtained from the direct application of Equations (1) to (4) presented in Section 2. The graphic interface is normally composed of the input fields, according to the number of parameters, and by one output field linked to the final vulnerability map. In the case of SINTACS, the last functionality opens a window (Figure 3) with six options according to Civita [20,21].

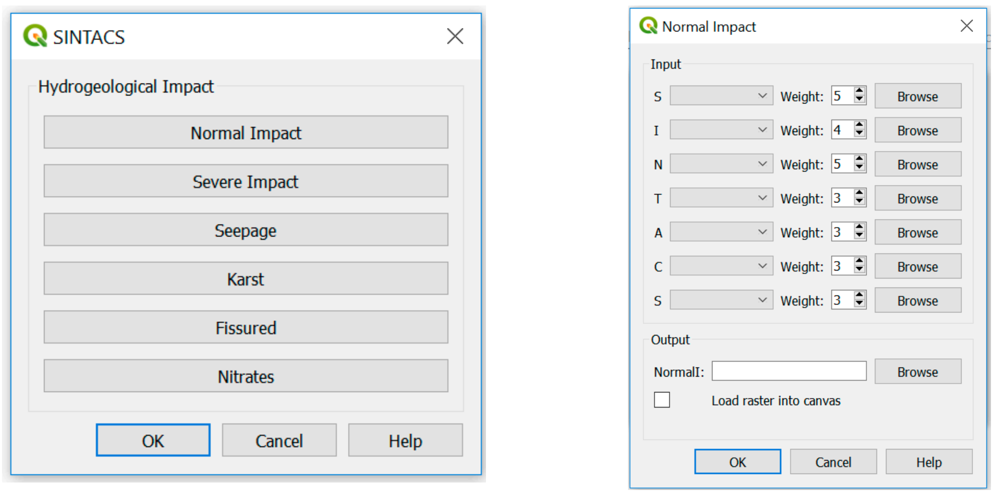

(a) **(b)**

Figure 3. SINTACS windows: type of hydrogeological impact (**a**) and weights of the *Normal Impact* option (**b**).

In this window Figure 3b the user must choose the adequate impact according to the knowledge of the study area. Then, a new window shows up with the predefined weights and the input and output fields (Figure 3). The weights can be also modified by the user.

3.8. *Comparative Analysis Menu Implementation*

The *Comparative Analysis* menu was created to carry out an enhanced side-by-side vulnerability map comparison by subtracting pixel values from two raster maps with normalized index values.

It is composed of two input fields, and four spin boxes with predefined values corresponding to the minimum and maximum values of raster and the minimum and maximum values of the normalization interval, and one output field. Since each final map has different index scales and intervals, the functionality was automatized with a process of normalization of the predefined set of values in each map. A spin box was created to perform this possibility of selection. The normalization was implemented through *r.rescale* algorithm from Geographic Resources Analysis Support System (GRASS). The comparative map provides the differences between two indices. The greater the absolute value for every pixel of the comparative map, the greater the contrast of groundwater vulnerability. To perform the differences, the *r.mapcalc.simple* algorithm from GRASS was implemented in the functionality.

3.9. Map Statistics

The *Map Statistics* menu was also incorporated in the *GVTool*, with a functionality through which the user can define the input vulnerability map and the output file with the computed statistics (minimum, maximum, mean, standard deviation, and range of index values). This implementation was based on *rasterlayerstatistics* algorithm from QGIS. The output file of this algorithm is an html file. However, this functionality has an option to create the statistic variables in a word pad file through a check box option.

3.10. Apply Symbology

Through the *Apply Symbology* menu, the user may define new vulnerability classes (by defining new index intervals) and apply a specific symbology to a certain vulnerability map or group of maps. This procedure is useful to compare different vulnerability maps using harmonized classes (Figure 4). To implement this functionality, a table was created, with predefined classes for each index, using *QTableWidget* module.

The first group of this functionality is composed of a table including the four implemented methods and the respective predefined vulnerability classes. The user can change these values or keep the default ones. In the second line of the table, the user finds a combo box, which allows one to choose the raster file (which must be open in QGIS canvas). The check boxes are intended for selecting the maps to which the new index classes and symbology will be applied. The output field allows one to save a *.qml* file with the style saved.

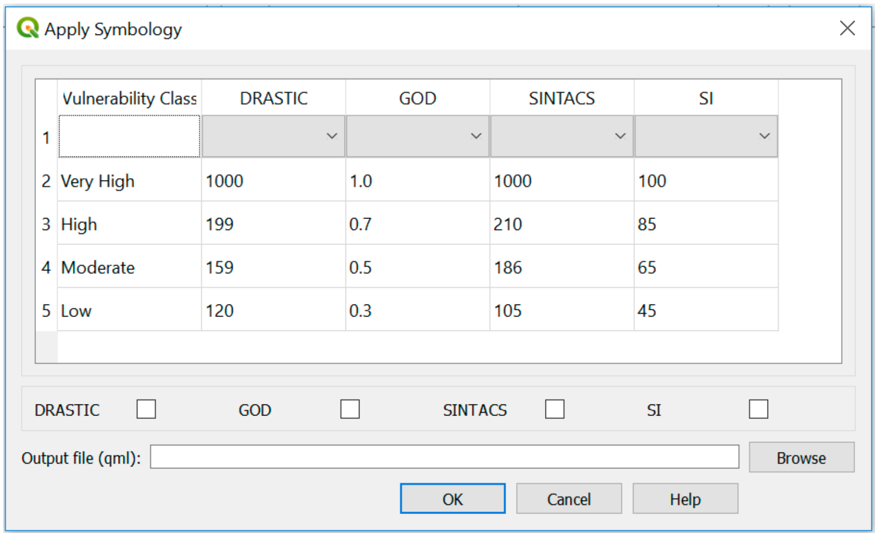

Figure 4. Symbology window.

4. *GVTool* Illustrative Application

In this section, we illustrate the *GVTool* application and performance in a study area in order to highlight the applications' ability to assess groundwater vulnerability to pollution. A possible workflow is presented; however, *GVTool* could be employed in many different ways, depending on the hydrogeological features of each study area, as well as on the user requirements.

The study area is a sector from Serra da Estrela mountain (Central Portugal) ,which was chosen to illustrate the application of *GVTool* given its demanding groundwater vulnerability assessment conditions, particularly the complexity of the respective hydrogeological system and the data scarcity concerning some vulnerability factors, as explained in the following sections.

4.1. Hydrogeological Framework

The *GVTool* was tested in a sector of Serra da Estrela mountain (40° 15–38′ N; 7° 18–47′ W), Central Portugal, with an area of 116.9 km^2, and an altitude ranging from 875 m in Manteigas town to 1993 m at the Torre summit, which is the highest point on the Portuguese mainland (Figure 5).

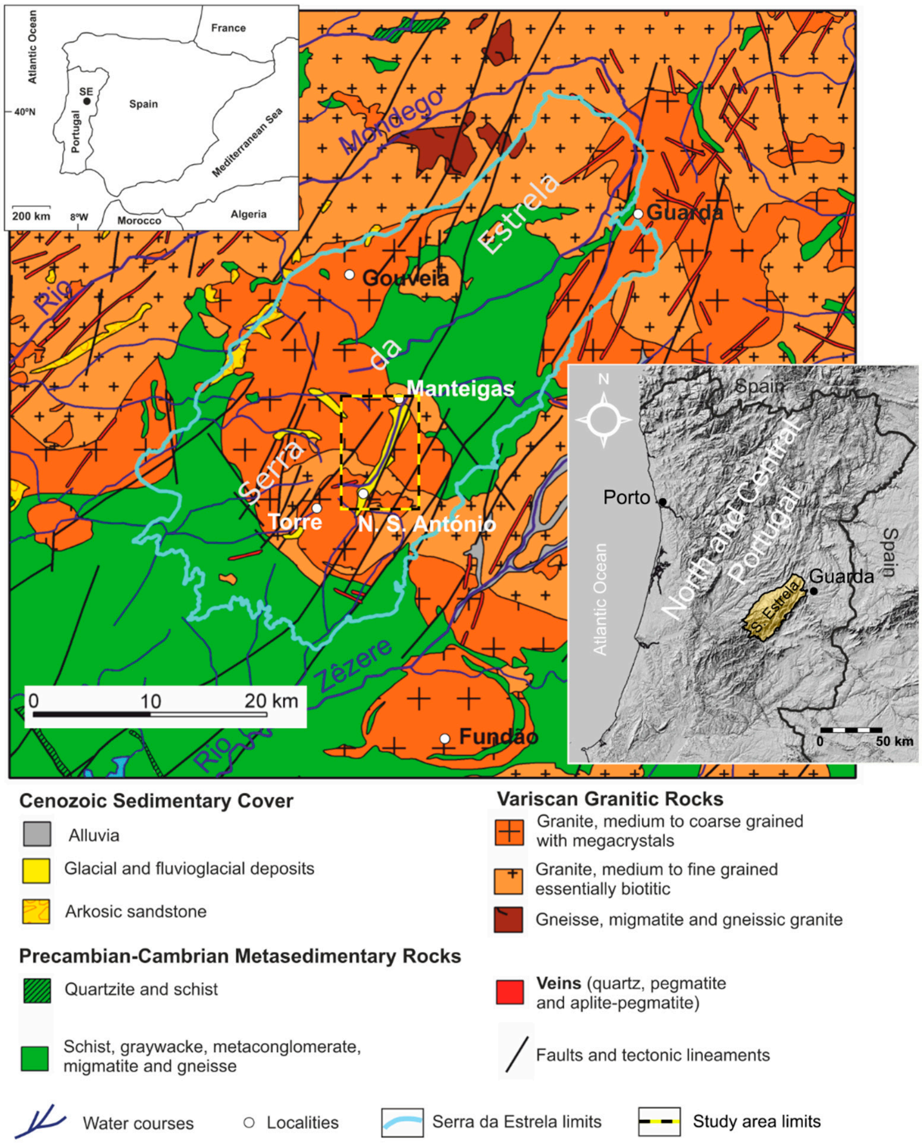

Figure 5. Geological setting of Serra da Estrela mountain and location of the study area.

Serra da Estrela is located in the Central-Iberian Zone of the Iberian Massif and the most important tectonic structure is the NNE-SSW Bragança-Vilariça-Manteigas fault zone. The main geological units are Variscan granitic rocks, Pre-Cambrian metasedimentary rocks and Cenozoic Sedimentary Cover, alluvia, and glacial deposits.

The Serra da Estrela climate is typically Mediterranean, but, to the northwest (NW), an Atlantic influence prevails [55,56]. According to Iberian Climate Atlas (AEMET-IM) [57], these climatic features are also expressed by the Köppen-Geiger classification, since the south-eastern (SE) part of the mountain is mainly of the climate subtype Csa (warm temperate, with dry and hot summers), while in the north-western area the climatic subtype is Csb (warm temperate, with dry and warm summers).

The mean annual precipitation is around 2500 mm in the highest areas of Serra da Estrela. On the western side of the mountain the total precipitation is lower than that on the eastern side, and it increases with elevation [58]. The data concerning snow precipitation is scarce. The mean annual air temperature is less than 7 °C in the upper part of the mountain and is less than 4 °C at the vicinity of the Torre summit [59].

According to Espinha Marques et al. [60,61], the dominant soils at the studied sector are: (i) Humic, Leptic, and Skeletic Umbrisols; (ii) Lithic and Umbric Leptosols; (iii) Umbric Fluvisols; and (iv) Rock outcrops. These soils are coarse textured, acidic, with high humified organic matter content, and the typical soil profile is ACR (A: A horizon; C: C horizon; R: hard bedrock) with an umbric A horizon.

The conditions of the local hydrogeological cycle conditions are mainly determined by the geological, tectonic, pedological, and climatic features, typical of a Mediterranean mountain region. As for groundwater circulation, fractured media exist in poorly weathered granitic and metasedimentary rocks and porous media are dominant in alluvia and quaternary glacial deposits, as well as in the most weathered granites and metasedimentary rocks [61].

Urban and agricultural pollution sources are limited to Manteigas town and its vicinity. However, other pollution sources are more widespread throughout the study region: (i) groundwater and surface water pollution resulting from road de-icing operations, namely, due to the use of NaCl and $CaCl_2$ as de-icing agents in the roads that cross the mountain and reach the Torre summit [62] and; (ii) the impact of wildfire on water bodies, consisting, mainly, of the pollution of aquifers, streams, and ponds caused by pyrogenic polycyclic aromatic hydrocarbons resulting from vegetation combustion [63].

4.2. Application of GVTool to The Region of Serra da Estrela

Serra da Estrela mountain corresponds to a protected area where some types of data are scarce or inexistent, such as information regarding depth to water table. The most relevant available data are presented in Table 2.

Table 2. Data available in the study zone.

Description	Source	Coordinate System	Resolution(m)/Scale
Digital Elevation Model (DEM)	Shuttle Radar Topography Mission (SRTM) [64]	European Terrestrial Reference System 1989—Portugal Transverse Mercator 2006 (ETRS89 PTTM06)	30
Geological map of Serra da Estrela Natural Park	National Laboratory of Energy and Geology [65]	Hayford Gauss militar, datum Lisboa	1/75,000
Land Cover map (Corine Land Cover—CLC)	Land General Direction (*Direção Geral do Território*, DGT [46])	European Terrestrial Reference System 1989—Portugal Transverse	20

Firstly, the *GVTool* was applied to the study area (the Manteigas-Torre sector, Figure 5) through an approach that consisted of selecting the most suitable ranges and ratings of each groundwater vulnerability factor for each groundwater vulnerability assessment method (Table 3). This selection was based on hydrogeological research carried out in recent years in Serra da Estrela. For this purpose, the hydrogeological conceptual model presented by Espinha Marques et al. [61] was particularly relevant. Then, a map for each factor was generated and the final output consisted of four groundwater vulnerability maps, expressing the results according to the DRASTIC, GOD, SINTACS, and SI methods (Figure 6).

The maps obtained following this procedure applied index intervals in accordance with previous studies, namely, Aller et al. [16] for DRASTIC, Foster et al. [17] for GOD, Al Kuisi et al. [47] for SINTACS, and Stigter et al. [25] for SI. These maps (Figure 6) are more suitable to represent the overall spatial distribution of groundwater vulnerability in the case of DRASTIC, SINTACS, and SI, and are less appropriate in the case of GOD. In fact, given the hydrogeological conditions of the Manteigas-Torre sector (e.g., Espinha Marques et al. [61]) the GOD index map oversimplifies the spatial distribution of groundwater vulnerability, since it represents homogeneous areas encompassing very different conditions (for example, valley bottoms and slopes), which is not realistic.

Table 4 presents fundamental statistics for each vulnerability index using the *GVTool Map Statistics* functionality.

Table 3. DRASTIC, GOD, SINTACS, and SI factors selected for the Serra da Estrela Study area.

	Hydrogeological Units		
	Sedimentary Cover	**Granitic Rocks**	**Metasedimentary Rocks**
D	estimated through spatial interpolation		
R	estimated through spatial interpolation		
A	sand and gravel	igneous rocks	metamorphic rocks
S	sand	sand	Loam
T	estimated through spatial interpolation		
I	sand and gravel	igneous rocks	metamorphic rocks
C	10^{-2} cm/s	10^{-4} cm/s	10^{-4} cm/s
G	unconfined	unconfined	unconfined
O	alluvial and fluvioglacial sands	igneous formations	metamorphic formations
D	estimated through spatial interpolation		
S	estimated through spatial interpolation		
I	estimated through spatial interpolation		
N	coarse alluvial deposit	fissured plutonic rock	fissured metamorphic rock
T	sandy	sandy	loam
A	coarse alluvial deposit	fissured plutonic rock	fissured metamorphic rock
C	10^{-2} cm/s	10^{-4} cm/s	10^{-4} cm/s
S	estimated through spatial interpolation		
D	estimated through spatial interpolation		
R	estimated through spatial interpolation		
A	sand and gravel	sand and gravel	sand and gravel
T	estimated through spatial interpolation		
LU	factor rating assigned according to the land use class		

Table 4. Statistics from DRASTIC, GOD, SINTACS, and SI vulnerability index maps.

	DRASTIC	**GOD**	**SINTACS**	**SI**
Min	67.00	0.45	130.50	31.52
Max	183.00	0.63	251.50	87.15
Mean	122.19	0.53	173.55	41.81
Standard Deviation (SD)	14.98	0.04	32.22	7.35
Range	116.00	0.17	121.00	55.63
Coefficient of Variation (CV)	0.12	0.08	0.19	0.18

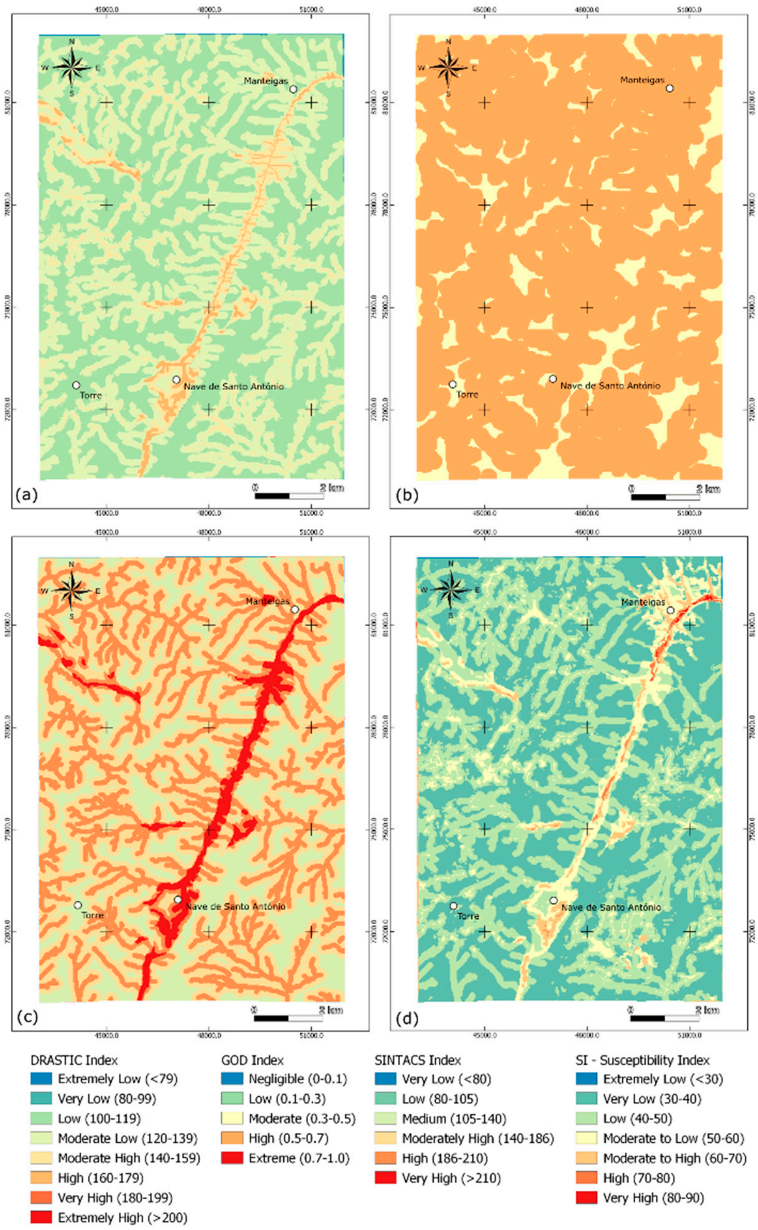

Figure 6. Groundwater vulnerability maps from the Manteigas-Torre Sector (Serra da Estrela), calculated using index intervals from previous studies: DRASTIC (**a**), GOD (**b**), SINTACS (**c**), and SI (**d**).

In the second stage, in order to make vulnerability maps more comparable, a uniform vulnerability classification was defined according to a procedure presented by Lobo Ferreira and Oliveira [66]. These authors highlighted the difficulty of comparing vulnerability maps representing values from different vulnerability indices (each one with its own vulnerability classes). The accuracy of this procedure is greatly improved by defining the same set of vulnerability classes for all methods. For this purpose, four vulnerability classes were defined (Table 5), using the *Apply Symbology* window: (i) Low, (iii) Moderate, (iv) High, and (v) Very High.

From the maps presented in Figures 6 and 7, we can conclude that: (i) generally, DRASTIC, SINTACS, and SI present more realistic results than GOD; (ii) DRASTIC, SINTACS, and SI are more sensitive than GOD to the spatial impacts of geology, topography, and depth to water table in groundwater vulnerability; and (iii) the application of SI for creating the maps from Figures 6d and 7d represents an important improvement over the maps from DRASTIC, GOD, and SINTACS because, due to the inclusion of the LU factor, this method is able to represent the influence on groundwater vulnerability of agricultural and urban land use classes, along with classes corresponding to protected areas from Serra da Estrela Natural Park.

Since DRASTIC, SINTACS, and SI assess groundwater vulnerability through a larger variety of factors, the respective maps are more capable of representing subtler spatial variations than the ones obtained using GOD index. This effect is particularly evident in the second set of vulnerability maps (Figure 7), obtained with similar vulnerability index intervals. Moreover, these vulnerability maps express more clearly a shift of SINTACS results towards higher vulnerability values when compared to DRASTIC and SI.

Table 5. Reclassified index intervals for the Manteigas-Torre sector.

Vulnerability Class	DRASTIC	GOD	SINTACS	SI
Very high	>199	0.7–1.0	>210	85–100
High	160–199	0.5–0.7	186–210	65–85
Moderate	120–159	0.3–0.5	105–186	45–65
Low	<120	0.0–0.3	<105	0–45

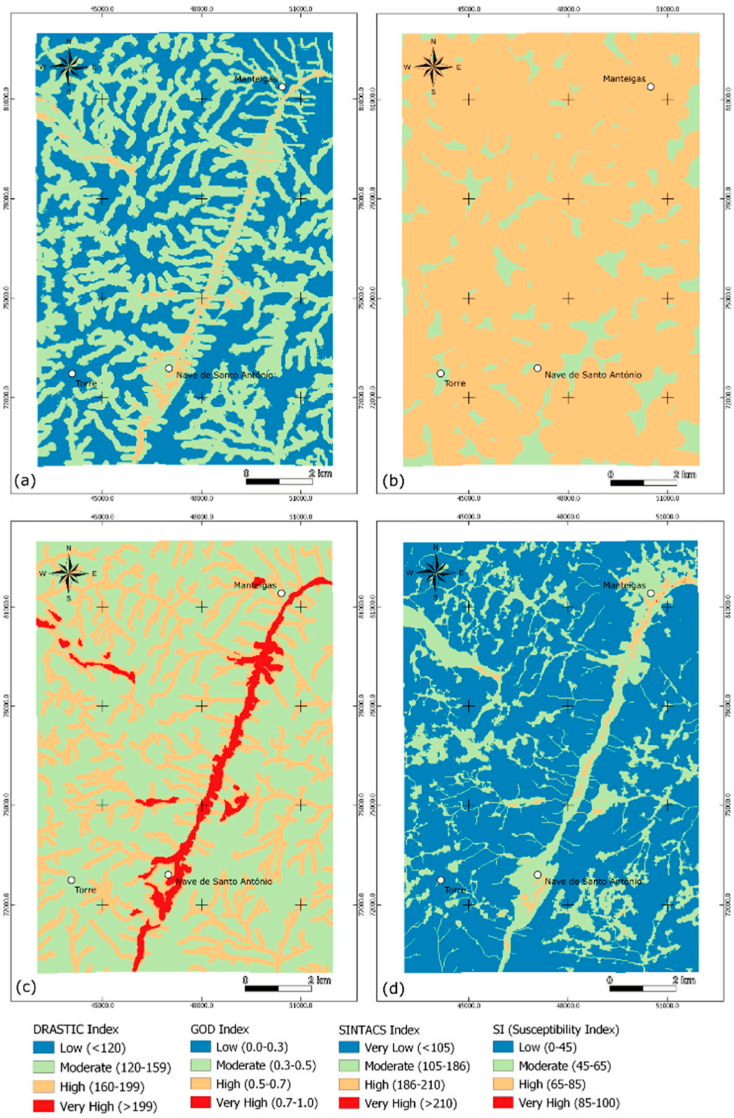

Figure 7. Groundwater vulnerability maps from the Manteigas-Torre Sector (Serra da Estrela), calculated using reclassified index intervals: DRASTIC (**a**), GOD (**b**), SINTACS (**c**), and SI (**d**).

Given the results of the earlier stages of the application of *GVTool* to the Manteigas-Torre sector, the functionalities of the *Comparative Analysis* menu were applied in order to compare different pairs of vulnerability maps where the value of each pixel was calculated from the subtraction of normalized index values, from 0 to 100 (Figure 8).

The (DRASTIC-SINTACS) comparative map (Figure 8) points out that the results are, in general terms, quite analogous, as should be expected from methods based on similar sets of vulnerability factors. Indeed, both methods tend to deliver higher vulnerability values in areas close to streams and valley bottoms (as illustrated by Figure 7a,b), where the water table is shallower, and slopes are less steep. However, Figure 8 shows that DRASTIC values are generally higher than SINTACS, especially in steeper slopes and in convex landforms, such as summits and crests. On the contrary, SINTACS values tend to be higher than DRASTIC along the main valley bottom and some of its tributaries.

In most of the study area, the DRASTIC-SI comparative map (Figure 8) shows that DRASTIC computes higher vulnerability than SI, especially in steeper slopes and convex landforms. However, the effect of the LU factor from SI index is quite noticeable in the northeast (NE) part of the map, in the Manteigas town area, where urban and agricultural land use prevail, and a greater balance between DRASTIC and SI index values is represented.

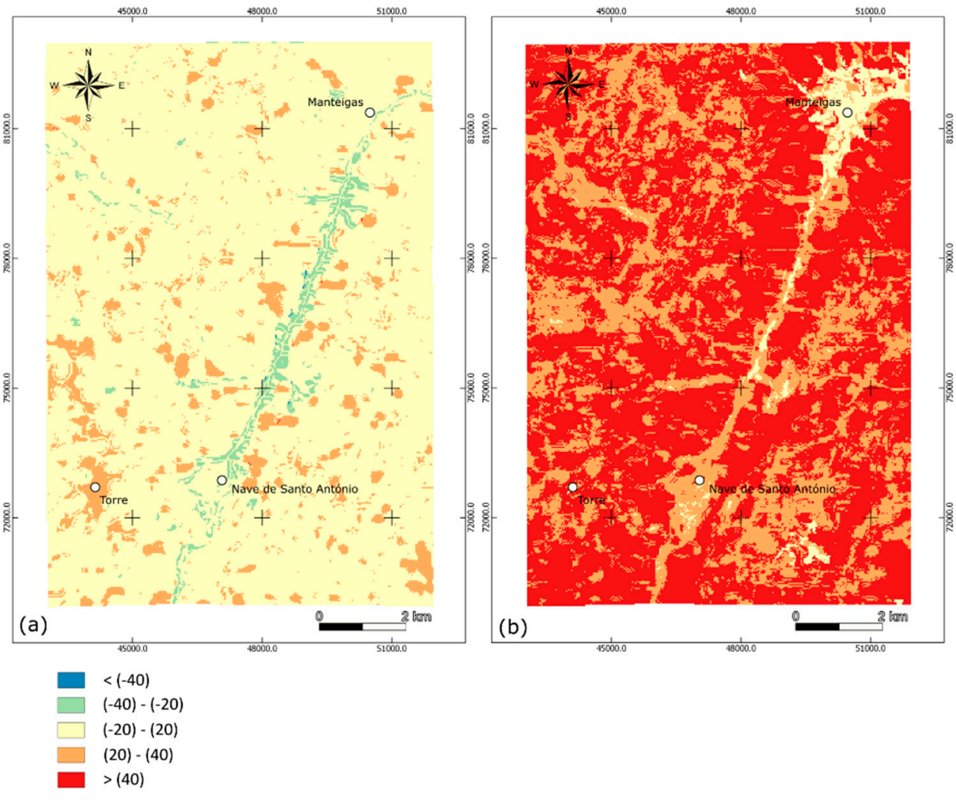

Figure 8. Comparative groundwater vulnerability maps from the Manteigas-Torre Sector (Serra da Estrela), calculated using normalized index values: DRASTIC-SINTACS (**a**) and DRASTIC-SI (**b**).

The application of *GVTool* to the Manteigas-Torre sector has shown that some methods are more adequate for assessing and mapping groundwater vulnerability in this region than others. Several types of map comparisons were carried out, starting with side-by-side visual map comparisons. In order to reduce the subjectivity of this procedure, other comparisons were made in subsequent stages using the functionalities *Apply Symbology* and *Comparative Analysis*. These comparisons revealed that DRASTIC, SINTACS, and SI perform better than GOD when applied to this study area.

The overall vulnerability values tend to be lower in the SI map, intermediate in the DRASTIC map, and higher in the SINTACS map. In order to strictly represent the intrinsic groundwater vulnerability, DRASTIC is the most balanced choice. However, the representation of the influence of specific urban and agricultural land use classes is only achieved by means of the SI map.

5. Conclusions

The sustainable management of water resources at different scales requires mapping tools, namely, GIS-based tools, which are crucial for improving the decision-making processes involving water users, private companies, public institutions, and authorities. Groundwater vulnerability maps are fundamental for spatial planning, since these instruments may be used to identify, and if necessary, to protect the most sensitive areas, for instance, by removing or preventing the installation of potentially pollutant economic activities. *GVTool* is a new GIS-based groundwater vulnerability assessment tool developed under QGIS, a free and open source application, with the purpose of providing a friendly and accurate application for creating and comparing groundwater vulnerability maps using four well-established methods: DRASTIC, GOD, SINTACS, and SI. *GVTool* can be improved, modified by any user, or even adapted to different hydrogeological contexts in different regions. This possibility enhances the usability of *GVTool* in the open source software context, since it is friendly and intuitive, and it is available to any user of any scientific area, familiarized or not with GIS software. The application of different vulnerability assessment methods to a certain study area will often produce contrasting results, and consequently, the comparison of different vulnerability maps is a central issue in the application of *GVTool*. Using different groundwater vulnerability assessment methods may result in contrasting maps, expressing different spatial distributions of vulnerability index values and classes. *GVTool* has the capability of helping to identify the most appropriate methods for a particular study area, and even to decide if the best choice is to create a composite vulnerability map.

The *GVTool* workflow may be easily adapted to the hydrogeological features of each study region. With the purpose of illustrating the *GVTool* functionalities and capabilities, a groundwater vulnerability assessment was carried out in the Manteigas-Torre sector. Side-by-side map comparisons were performed, which highlighted the way specific vulnerability factors influence the computed index values. Additionally, *GVTool* helped perceive if each method tended to shift index values towards higher or lower vulnerability classes. The application may also be very useful in integrated assessments, allowing multidisciplinary and interdisciplinary approaches and helping researchers to choose the best method or combination of methods to express groundwater vulnerability to pollution.

In order to address some limitations of the present *GVTool* version, the application will be improved with further functionalities, such as: (i) the addition of groundwater vulnerability assessment methods more suitable for fractured and karstic environments; (ii) to increase *GVTool* flexibility by providing the user the possibility of modifying the implemented indices, and even to create their own index, i.e., the user can compose the index with the parameters, weights, and ratings better adjusted to the study area characteristics; (iii) the addition of a functionality dedicated to combining two or more ordinary vulnerability maps into a composite vulnerability map; and (iv) to couple *GVTool* with a new GIS-based tool, dedicated to delineating wellhead protection areas (this tool will be implemented by the authors in the near future).

GVTool is free, open source, and available at http://www.fc.up.pt/pessoas/liaduarte/GVTool.rar.

Author Contributions: Conceptualization, A.C.T., L.D., and J.E.M.; methodology, J.E.M.; software, L.D.; validation, J.E.M.; formal analysis, J.E.M.; investigation, A.C.T., L.D., and J.E.M.; resources, J.E.M.; writing—original draft preparation, A.C.T., L.D., and J.E.M.; writing—review and editing, A.C.T., L.D., and J.E.M.

Acknowledgments: This work was co-financed by European Union through the European Regional Development Fund, framed in COMPETE 2020 (Operational Programme for Competitiveness and Internationalization), through the project ICT (UID/GEO/04683/2013) with reference POCI-01-0145-FEDER-007690.

Conflicts of Interest: The authors declare no conflict of interest.

References

1. Ross, A. Groundwater Governance in Australia, the European Union and the Western USA. In *Integrated Groundwater Management: Concepts, Approaches and Challenges*; Jakeman, A.J., Barreteau, O., Hunt, R.J., Rinaudo, J., Ross, A., Eds.; Springer: Cham, Switzerland, 2016. [CrossRef]
2. Margat, J.; van der Gun, J. *Groundwater around the World, A Geographic Synopsis*; CRC Press: Boca Raton, FL, USA, 2013; ISBN 978-0-203-77214-0.
3. Nwankwoala, H.O. Groundwater and Poverty Reduction: Challenges and Opportunities for Sustainable Development in Nigeria. *Hydrol. Curr. Res.* **2016**, *7*, 2. [CrossRef]
4. EC. *Directive 2000/60/EC of the European Parliament and of the Council Establishing a Framework for Community Action in the Field of Water Policy*; OJ L 327, 22 December 2000; Office for Official Publications of the European Communities: Luxembourg, 2000.
5. EC. *Directive 2006/118/EC of the European Parliament and of the Council on the Protection of Groundwater Against Pollution and Deterioration*; OJ L 372, 27 December 2006; Office for Official Publications of the European Communities: Luxembourg, 2006.
6. Navarrete, C.M.; Olmedo, J.G.; Valsero, J.J.D.; Gómez, J.D.G.; Espinar, J.A.L.; Gómez, J.A.O. Groundwater protection in Mediterranean countries after the European water framework directive. *Environ. Geol.* **2008**, *54*, 537–549. [CrossRef]
7. Hérivaux, C.; Grémont, M. Valuing a diversity of ecosystem services: The way forward to protect strategic groundwater resources for the future? *Ecosyst. Serv.* **2019**, *35*, 184–193. [CrossRef]
8. Wachniew, P.; Zurek, A.J.; Stumpp, C.; Gemitzi, A.; Gargini, A.; Filippini, M.; Rozanski, K.; Meeks, J.; Kværner, J.; Witczak, S. Toward operational methods for the assessment of intrinsic groundwater vulnerability: A review. *Crit. Rev. Environ. Sci. Technol.* **2016**, *46*, 827–884. [CrossRef]
9. Shende, S.; Chau, K. Forecasting Safe Distance of a Pumping Well for Effective Riverbank Filtration. *J. Hazard. Toxic Radioact. Waste* **2019**, *23*. [CrossRef]
10. Van Duijvenbooden, W.V.; Waegeningh, H.G. Vulnerability of Soil and Groundwater to Pollutants. In *Proceedings and Information No. 38 of International Conference Held in the Netherlands*; TNO Committee on Hydrological Research: Delft, The Netherlands, 1987.
11. Krogulec, E. Intrinsic and Specific Vulnerability of Groundwater in a River Valley—Assessment, Verification and Analysis of Uncertainty. *Earth Sci. Clim. Chang.* **2013**, *4*. [CrossRef]
12. Vrba, J.; Zaporozec, A. *Guidebook on Mapping Groundwater Vulnerability, IAH, International Contributions to Hydrogeology, 16*; Heise: Hannover, Germany, 1994.
13. Lai, Y.; Wang, F.; Zhang, Y.; Li, S.; Wu, P.; Ou, P.; Fang, Q.; Chen, Z.; Duan, Y. Implementing chemical mass balance model and vulnerability the theories to realize the comprehensive evaluation in an abandoned battery plant. *Sci. Total Environ.* **2019**, *686*, 788–796. [CrossRef]
14. Kong, M.; Zhong, H.; Wu, Y.; Liu, G.; Xu, Y.; Wang, G. Developing and validating intrinsic groundwater vulnerability maps in regions with limited data: A case study from Datong City in China using DRASTIC and Nemerow pollution indices. *Environ. Earth Sci.* **2019**, *78*, 262. [CrossRef]
15. Machiwal, D.; Jha, M.K.; Singh, V.P.; Mohan, C. Assessment and mapping of groundwater vulnerability to pollution: Current status and challenges. *Earth-Sci. Rev.* **2018**, *185*, 901–927. [CrossRef]
16. Aller, L.; Bennett, T.; Lehr, J.H.; Petty, R.J.; Hackett, G. *DRASTIC: A Standardized System for Evaluating Ground Water Pollution Potential Using Hydrogeologic Settings*; EPA-600/2-87-035; EPA: Washington, DC, USA, 1987.
17. Foster, S.; Hirata, R.; Gomes, D.; Delia, M.; Paris, M. *Groundwater Quality Protection: A Guide for Water Utilities, Municipal Authorities, and Environment Agencies*; The International Bank for Reconstruction and Development; The World Bank: Washington, DC, USA, 2002.
18. Moore, P.; John, S. *SEEPAGE: A System for Early Evaluation of the Pollution Potential of Agricultural Groundwater Environments*; Geology Technical Note; USDA, SCS, Northeast Technical Center: Chester, PA, USA, 1990.
19. Van Stempvoort, D.; Ewert, L.; Wassenaar, L. Aquifer vulnerability index: A GIS-compatible method for groundwater vulnerability mapping. *Can. Water Resour. J.* **2013**, *18*, 25–37. [CrossRef]
20. Civita, M. *Le Carte Della Vulnerabilita Degli acquiferiall'inquinamento Teoria and Practica (Aquifer Vulnerability Maps to Pollution)*; Pitagora Editrice: Bologna, Italy, 1994.

21. Civita, M.; De Maio, M. *SINTACS Un Sistema Parametrico per la Valutazione e la Cartografia per la Valutazione Della Vulnerabilita'Degli Acquiferi All'inquinamento, Metodologia e Automazione*; Pitagora Editrice: Bologna, Italy, 1997.
22. Doerfliger, N.; Zwahlen, F. EPIK: A new method for outlining of protection areas in karst environment. In Proceedings of the 5th International Symposium and Field Seminar on Karst Waters and Environmental Impacts, Antalya, Turkey, 10–20 September 1995; Gunay, G., Johnson, I., Eds.; Balkema: Rotterdam, The Netherlands, 1995; pp. 117–123.
23. Civita, M.; De Regibus, C. Sperimentazione di alcune metodologie per la valutazione della vulnerabilita degli aquifer. *Quad. Geol. Appl.* **1995**, *3*, 63–72.
24. Davis, A.D.; Long, A.J.; Wireman, M. KARSTIC: A sensitivity method for carbonate aquifers in karst terrain. *Environ. Geol.* **2002**, *42*, 65–72. [CrossRef]
25. Stigter, T.Y.; Ribeiro, L.; Dill, A.M. Evaluation of an intrinsic and a specific vulnerability assessment method in comparison with groundwater salinisation and nitrate contamination levels in two agricultural regions in the south of Portugal. *Hydrogeol. J.* **2006**, *14*, 79–99. [CrossRef]
26. Jarray, H.; Zammouri, M.; Ouessar, M.; Zerrim, A.; Yahyaoui, H. GIS based DRASTIC Model for Groundwater Vulnerability Assessment: Case Study of the Shallow Mio-Plio Quaternary Aquifer (Southeastern Tunisia). *Water Resour.* **2017**, *44*, 595–603. [CrossRef]
27. Edet, A. An aquifer vulnerability assessment of the Benin Formation aquifer, Calabar, southeastern Nigeria, using DRASTIC and GIS approach. *Environ. Earth Sci.* **2014**, *71*, 1747–1765. [CrossRef]
28. Asadi, P.; Ataie-Ashtiani, B.; Beheshti, A. Vulnerability assessment of urban groundwater resources to nitrate: The case study of Mashhad, Iran. *Environ. Earth Sci.* **2017**, *76*, 41. [CrossRef]
29. Meerkhan, H.; Teixeira, J.; Espinha Marques, J.; Afonso, M.J.; Chaminé, H.I. Delineating Groundwater Vulnerability and Protection Zone Mapping in Fractured Rock Masses: Focus on the DISCO Index. *Water* **2016**, *8*, 462. [CrossRef]
30. Draoui, M.; Vias, J.; Andreo, B.; Targuisti, K.; Stitou El Messari, J. A comparative study of four vulnerability mapping methods in a detritic aquifer under mediterranean climatic conditions. *Environ. Geol.* **2007**, *54*, 455–463. [CrossRef]
31. Aschonitis, V.G.; Castaldelli, G.; Colombani, N.; Mastrocicco, M. A combined methodology to assess the intrinsic vulnerability of aquifers to pollution from agrochemicals. *Arab. J. Geosci.* **2016**, *9*, 503. [CrossRef]
32. Oroji, B. Groundwater vulnerability assessment using GIS-based DRASTIC and GOD in the Asadabad plain. *J. Mater. Environ. Sci.* **2018**, *9*, 1809–1816.
33. Yousefi, H.; Haghizadeh, A.; Yarahmadi, Y.; Hasanpour, P.; Noormohamadi, P. Groundwater pollution potential evaluation in Khorramabad-Lorestan Plain, western Iran. *J. Afr. Earth Sci.* **2018**, *147*, 647–656. [CrossRef]
34. Yildirim, M.; Topkaya, B. Groundwater Protection: A Comparative Study of Four Vulnerability Mapping Methods. *Clean* **2007**, *35*, 594–600.
35. Saida, S.; Tarik, H.; Abdellah, A.; Farid, H.; Hakiml, B. Assessment of Groundwater Vulnerability to Nitrate Based on the Optimised DRASTIC Models in the GIS Environment (Case of Sidi Rached Basin, Algeria). *Geosciences* **2017**, *7*, 20. [CrossRef]
36. Pisciotta, A.; Cusimano, G.; Favara, R. Groundwater nitrate risk assessment using intrinsic vulnerability methods: A comparative study of environmental impact by intensive farming in the Mediterranean region of Sicily, Italy. *J. Geochem. Explor.* **2015**, *156*, 89–100. [CrossRef]
37. Stallman, P. Why 'Open Source' Misses the Point of Free Software, GNU Operating System. Available online: http://www.gnu.org/philosophy/open-sourcemisses-the-point.html (accessed on 10 February 2019).
38. QGIS Project. Available online: http://www.qgis.org/ (accessed on 10 November 2018).
39. Groundwater Vulnerability Mapping Plugin, Hosted in QGIS Official Repository (from Christian Boehnke). Available online: https://plugins.qgis.org/plugins/GroundwaterVulnerability/ (accessed on 10 June 2019).
40. Ollivier, C.; Lecomte, Y.; Chalikakis, K.; Mazzilli, N.; Danquigny, C.; Emblanch, C. A QGIS Plugin Based on the PaPRIKa Method for Karst Aquifer Vulnerability Mapping. *Groundwater* **2019**, *57*, 201–204. [CrossRef]
41. Rossetto, R.; De Filippis, G.; Borsi, I.; Foglia, L.; Cannata, M.; Criollo, R.; Vázquez-Suñé, E. Integrating free and open source tools and distributed modelling codes in GIS environment for data-based groundwater management. *Environ. Model. Softw.* **2018**, *107*, 210–230. [CrossRef]

42. Duarte, L.; Teodoro, A.C.; Gonçalves, J.A.; Guerner Dias, A.J.; Espinha Marques, J. A dynamic map application for the assessment of groundwater vulnerability to pollution. *Environ. Earth Sci.* **2015**, *74*, 2315–2327. [CrossRef]
43. Processing Toolbox. Available online: https://github.com/qgis/QGIS/wiki/Plugin-migration-to-QGIS-3 (accessed on 10 March 2019).
44. Afonso, M.J.; Freitas, L.; Pereira, A.J.S.C.; Neves, L.J.P.F.; Guimarães, L.; Guilhermino, L.; Mayer, B.; Rocha, F.; Marques, J.M.; Chaminé, H.I. Environmental Groundwater Vulnerability Assessment in Urban Water Mines (Porto, NW Portugal). *Water* **2016**, *8*, 499. [CrossRef]
45. Ouedraogo, I.; Defourny, P.; Vanclooster, M. Mapping the groundwater vulnerability for pollution at the pan African scale. *Sci. Total Environ.* **2016**, *544*, 939–953. [CrossRef]
46. Foster, S.S.D. Fundamental concepts in aquifer vulnerability, pollution risk and protection strategy. In *Vulnerability of Soil and Groundwater to Pollution*; Proceedings and Information No. 38 of the International Conference held in the Netherlands, in 1987; van Duijvanbooden, W., van Waegeningh, H.G., Eds.; TNO Committee on Hydrological Research: Delft, The Netherlands, 1987.
47. Al Kuisi, M.; El-Naqa, A.; Hammouri, N. Vulnerability mapping of shallow groundwater aquifer using SINTACS model in the Jordan Valley area, Jordan. *Environ. Geol.* **2006**, *50*, 651. [CrossRef]
48. Francés, A.; Paralta, E.; Fernandes, J.; Ribeiro, L. Development and application in the Alentejo region of a method to assess the vulnerability of groundwater to diffuse agriculture pollution: The susceptibility index. In Proceedings of the Third International Conference on Future Groundwater Resources at Risk, Lisbon, Portugal, 25–27 June 2001; GeoSystem Center IST: Lisboa, Portugal, 2001.
49. DGT (Direção Geral do Território). Available online: http://www.dgterritorio.pt/dados_abertos/clc/ (accessed on 13 March 2019).
50. Bonham-Carter, G.F. Geographic Information Systems for Geoscientists, Modelling with GIS. *Comput. Method Geosci.* **1994**, *13*, 152–153.
51. Deutsch, C.; Journel, A. *GSLIB: Geostatistical Software Library and User's Guide*; Oxford University Press: Oxford, UK, 1992; p. 340.
52. Haber, J.; Zeilfelder, F.; Davydov, O.; Seidel, H.P. Smooth approximation and rendering of large scattered data sets. In Proceedings of the IEEE Visualization, San Diego, CA, USA, 21–26 October 2001; Joy, T.E.K., Varshney, A., Eds.; IEEE Computer Society: Washington, DC, USA, 2001; Volume 571, pp. 341–347.
53. Mitasova, H.; Mitas, L.; Brown, B.M.; Gerdes, D.P.; Kosinovsky, I. Modeling spatially and temporally distributed phenomena: New methods and tools for GRASS GIS. *Int. J. GIS Spec. Issue Integr. GIS Environ. Model* **1995**, *9*, 433–446.
54. Mitasova, H.; Mitas, L.; Harmon, R.S. Simultaneous spline approximation and topographic analysis for lidar elevation data in open source GIS. *IEEE GRSL* **2005**, *2*, 375–379. [CrossRef]
55. Jansen, J.; Sequeira, M.P.S.M. The vegetation of shallow waters and seasonally inundated habitats (Littorelletea and Isoeto-Nanojuncetea) in the higher parts of the Serra da Estrela, Portugal. *Mitt. Badischen Landesver. Naturkunde* **1999**, *17*, 449–462.
56. Mora, C. A synthetic map of the climatopes of the Serra da Estrela (Portugal). *J. Maps* **2010**, *6*, 591–608. [CrossRef]
57. AEMET-IM. *Iberian Climate Atlas, Air Temperature and Precipitation (1971–2000)*; Ministerio de Medio Ambiente, Medio Rural y Marino: Madrid, Spain, 2011.
58. Daveau, S.; Coelho, C.; Costa, V.G.; Carvalho, L. *Distribution and Rhythm of Precipitation in Portugal*; Memórias do Centro de Estudos Geográficos: Lisbon, Portugal, 1977. (In French)
59. Vieira, G.T.; Mora, C. General characteristics of the climate of the Serra da Estrela. In *Glaciar Periglacial Geomorphology of the Serra da Estrela, Guidebook for the Field-Trip*; IGU Commission on Climate Change and Periglacial Environments, 26–28 August 1998; Vieira, G.T., Ed.; CEG and Department of Geology, University of Lisbon: Lisbon, Portugal, 1998; pp. 26–36.
60. Espinha Marques, J.; Duarte, J.M.; Constantino, A.T.; Martins, A.A.; Aguiar, C.; Rocha, F.T.; Inácio, M.; Marques, J.M.; Chaminé, H.I.; Teixeira, J.; et al. Vadose zone characterisation of a hydrogeologic system in a mountain region: Serra da Estrela case study (Central Portugal). In *Aquifer Systems Management: Darcy's Legacy in a World of Impending Water Shortage*; SP-10 Selected papers on Hydrogeology; Chery, L., Marsily, G.D., Eds.; IAH, Taylor & Francis Group: London, UK, 2007; pp. 207–221.

61. Espinha Marques, J.; Marques, J.M.; Chaminé, H.I.; Carreira, P.M.; Fonseca, P.E.; Monteiro Santos, F.A.; Moura, R.; Samper, J.; Pisani, B.; Teixeira, J.; et al. Conceptualizing a mountain hydrogeologic system by using an integrated groundwater assessment (Serra da Estrela, Central Portugal): A review. *Geosci. J.* **2013**, *17*, 371–386. [CrossRef]
62. Espinha Marques, J.; Marques, J.M.; Carvalho, A.; Carreira, P.M.; Moura, R.; Mansilha, C. Groundwater resources in a Mediterranean mountainous region: Environmental impact of road de-icing. Sustain. *Water Resour. Manag.* **2019**, *5*, 305–317. [CrossRef]
63. Mansilha, C.; Carvalho, A.; Guimarães, P.; Marques, J.E. Water quality concerns due to forest fires: Polycyclic aromatic hydrocarbons (PAH) contamination of groundwater from mountain areas. *J. Toxicol. Environ. Health* **2014**, *77*, 806–815. [CrossRef]
64. SRTM (Shuttle Radar Topography Mission). Available online: https://earthdata.nasa.gov/nasa-shuttle-radar-topography-mission-srtm-version-3-0-global-1-arc-second-data-released-over-asia-and-australia (accessed on 3 January 2019).
65. LNEG (Laboratório Nacional de Energia e Geologia). Available online: http://geoportal.lneg.pt/geoportal/egeo/DownloadCartas/login.aspx (accessed on 3 January 2019).
66. Lobo Ferreira, J.P.; Oliveira, M.M. Groundwater vulnerability assessment in Portugal. *Geofís. Int.* **2004**, *43*, 541–550.